Formation of Mixed Fibrils Demonstrates the Generic Nature and Potential Utility of Amyloid Nanostructures

Cait E. MacPhee and Christopher M. Dobson*

Contribution from the Oxford Centre for Molecular Sciences, New Chemistry Laboratory, University of Oxford, South Parks Road, Oxford OX13QT, United Kingdom

Received August 8, 2000

Abstract: The aggregation of proteins and peptides in the form of stable and highly ordered amyloid fibrils is most commonly associated with pathological conditions such as Alzheimer's disease and the transmissible spongiform encephalopathies. The involvement of only a handful of proteins in amyloid formation in vivo has commonly been thought of as the result of some unusual conformational characteristic of the sequences of the proteins involved. Recent evidence has however suggested that the formation of these highly ordered structures is a generic process arising from the fundamental physicochemical properties of the polypeptide chain. In this study, we have shown that we can incorporate short peptides into amyloid fibrils assembled from unrelated peptides and from a full-length protein. This result provides compelling evidence that amyloid fibril assembly is a fundamental property of polypeptide chains. We have also demonstrated by doping with fluorescently labeled peptides that the fibrils can be modified to incorporate unusual functional groups, suggesting the possibility of the production of a wide range of novel nanomaterials with potentially important properties.

Introduction

A range of debilitating human diseases is associated with protein misfolding events. Recently, considerable attention has been focused on a group of diseases where proteins or fragments of proteins convert from their normally soluble forms to insoluble fibrils or plaques, which accumulate in a variety of organs including the liver, spleen, and brain.[1] The insoluble material, known as amyloid, has a well-defined fibrillar structure.[2] The diseases associated with amyloid deposition include Alzheimer's disease, the spongiform encephalopathies such as Creutzfeldt-Jakob disease and kuru, late-onset diabetes, and a range of less well-known but often equally serious conditions such as fatal familial insomnia and familial Mediterranean fever.[3] The formation and deposition of protein aggregates is thought to be the direct or indirect origin of the pathological conditions associated with the disease in question, and each disease is associated with a particular protein. Remarkably, despite the fact that all of the proteins involved in these diseases have unique and characteristic native folds, the fibrils in which they are found in the disease states are extremely similar in their overall appearance.[4] These supramolecular aggregates are characterized by a typical "cross-β" X-ray diffraction pattern indicative of a stacked β-sheet structure in which the strands are arranged perpendicular to the fibril axis; by a long, unbranched appearance under electron microscopy; and by staining with the dye Congo Red, which exhibits a green birefringence when viewed under polarized light.

The involvement of only a handful of proteins in amyloid diseases has commonly been thought to be the result of some particular conformational characteristic of the protein sequences involved. But evidence has recently accumulated suggesting that the ability to form amyloid fibrils is not a peculiarity of this small group of proteins.[5] At low pH, a concentrated solution of the SH3 domain of PI-3′ kinase turned into a viscous gel after several hours.[6] When this gel was examined by electron microscopy and other techniques, it was found to contain well-defined fibrils with all the characteristics of those associated with disease-related amyloid. This protein has no connection with any known disease. Formation of similar fibrils has also been observed when a domain of fibronectin was heated to temperatures above that required for unfolding.[7] Similarly, acylphosphatase was found to form amyloid fibrils when incubated under partially denaturing conditions[8] and other examples are being steadily reported. Interestingly, there are also a number of observations in the early literature of fibrous gels being formed for a range of different proteins under a variety of nonphysiological conditions,[9] reinforcing the idea that the ability to form amyloid fibrils is a generic property of polypeptide chains. This ability can readily be explained by the fact that the intermolecular bonds that stabilize this material involve the peptide backbone, which is common to all proteins. It also follows that if the formation of amyloid fibrils is a truly generic property of the peptide backbone, it should be possible to gen-

* Corresponding author: (tel) 44 1865 275919; (fax) 44 1865 275921; (e-mail) chris.dobson@chem.ox.ac.uk.

(1) Kelly, J. W. *Curr. Opin. Struct. Biol.* **1998**, *8*, 101−106. Lansbury, P. T. *Proc. Natl. Acad. Sci. U.S.A.* **1999**, *96*, 3342−3344. Perutz, M. F. *Trends Biochem. Sci.* **1999**, *24*, 58−63.

(2) Serpell, L. C.; Fraser, P. E.; Sunde M. *Methods Enzymol.* **1999**, *309*, 526−536.

(3) (a) Tateishi, J.; Brown, P.; Kitamoto, T.; Hoque, Z. M.; Roos, R.; Wollman, R.; Cervenakova, L.; Gajdusek, D. C. *Nature* **1995**, *376*, 434−435. (b) Grateau, G.; Drenth, J. P.; Delpech, M. *Curr. Opin. Rheumatol.* **1999**, *11*, 75−78.

(4) Serpell, L. C.; Fraser, P. E.; Sunde M. *Methods Enzymol.* **1999**, *309*, 526−536.

(5) Dobson, C. M. *Trends Biochem. Sci.* **1999**, *24*, 329−332.

(6) Guijarro, J. I.; Sunde, M.; Jones, J. A.; Campbell, I. D.; Dobson C. M. *Proc. Natl. Acad. Sci. U.S.A.* **1998**, *95*, 4224−4228.

(7) Litvinovich, S. V.; Brew, S. A.; Aota, S.; Akiyama, S. K.; Haudenschild, C.; Ingham, K. C. *J. Mol. Biol.* **1998**, *280*, 245−258.

(8) Chiti, F.; Webster, P.; Taddei, N.; Clark, A.; Stefani, M.; Ramponi, G.; Dobson, C. M. *Proc. Natl. Acad. Sci. U.S.A.* **1999**, *96*, 3590−3594.

(9) Tombs, M. P. *Faraday Discuss. Chem. Soc.* **1974**, *57*, 158−164.

10.1021/ja0029580 CCC: $19.00
Published on Web 12/27/2000

erate mixed fibrils comprising two independent molecular species.

In the present study, we demonstrate that amyloid fibrils consisting of two unrelated species can be formed. None of the peptides or proteins examined is directly implicated in any naturally occurring disease yet the resulting structures resemble closely those formed in vivo in pathological states. Furthermore, by incorporating extrinsic fluorescent groups into assembled fibrils, we demonstrate the assembly from protein molecules of well-defined fibrillar materials with unusual and potentially useful properties. Two peptides, TTR_{10-19} and $TTR_{105-115}$, both derived from the sequence of the human plasma protein transthyretin were employed in our investigations as probes of cofibril formation. Each corresponds to a β-strand in the native structure of this extensively β-sheet protein. Both peptides readily assemble into fibrils with all of the structural characteristics that are diagnostic of amyloid. TTR_{10-19} has a single cysteine residue at position 1 and this was chemically modified with the fluorophore fluorescein-5-maleimide (F5M-TTR_{10-19}). $TTR_{105-115}$ does not contain any amino groups other than the terminal α-amino group; this group was coupled to the fluorescent group dansyl chloride (dansyl-$TTR_{105-115}$).

Results

Incorporation of Labeled Peptides into "Self" Fibrils. To investigate whether chemical modification of the peptides interfered with the peptide self-assembly, we first formed amyloid fibrils containing a mixture of labeled and unlabeled peptides of the same amino acid sequence. After incubation for 7 days, the resulting fibrils were examined by ultracentrifugation, electron microscopy (EM), circular dichroism (CD) spectroscopy, and fluorescence methods. CD data were consistent with the formation of extensive β-sheet structure, and EM indicated the formation of fibrils that are visually very similar to those formed by the unlabeled peptides.[10] Sedimentation of the fibrils by ultracentrifugation resulted in partitioning of the fluorescent peptides almost exclusively into the fibrillar fraction, with less than 5% remaining in the supernatant. As shown in Figure 1A, the fluorescence emission of the fluorescein moiety of F5M-TTR_{10-19} undergoes a red-shift of 9 nm when incorporated into TTR_{10-19} fibrils, and the anisotropy of the fluorescein increases from 0.03 for the monomeric peptide in aqueous solution to 0.17 on formation of the fibrils (Table 1). This increase in the anisotropy of the fluorescent moiety indicates incorporation of the fluorophore into large complexes that exhibit slow rotational motion. The dansyl moiety of dansyl-$TTR_{105-115}$ exhibits a blue-shift of 26 nm when incorporated into fibrils comprising $TTR_{105-115}$ (Figure 1B) and an increase in the fluorescence anisotropy from 0.02 to 0.13 (Table 1).

Detection of Labeled Peptides in Peptide Cofibrils. These spectral changes provide a means of monitoring the incorporation of each of the two labeled peptides into fibrils composed predominantly of the other peptide. TTR_{10-19} containing 1% (w/w) dansyl-$TTR_{105-115}$ was resuspended at a final total peptide concentration of 10 mg/mL in 10% CH_3CN adjusted to pH 2 with TFA. The sample was incubated at 37 °C for 10 days, after which time the CD spectrum indicated the formation of significant β-sheet structure, and fibrils were observed by EM. The fluorescence spectrum shows a significant blue-shift in the emission from the dansyl moiety when compared to soluble peptide (Table 1), and the anisotropy of the probe increases from 0.03 to 0.17. Greater than 90% of the labeled peptide partitioned with the fibrils on sedimentation by ultracentrifugation. Fluorescence light microscopy of this pelleted material demonstrated a green fluorescence (Figure 2), consistent with insertion of the probe into high molecular weight structures. Similarly, 10 mg/mL $TTR_{105-115}$ containing only 1 wt % of F5M-TTR_{10-19} incubated for 10 days at 37 °C in 10% CH_3CN formed extensive β-sheet structure as indicated by CD. The shape of the CD spectrum is, however, substantially different from that of $TTR_{105-115}$ alone: a prominent negative band previously observed at ~235 nm, which we ascribe to the formation of a turn structure in the assembled fibrils, decreases in magnitude (Figure 3). This suggests a substantial change in the secondary structure of the peptides in the fibrillar array. The fibrils observed by EM are different in appearance from the almost crystalline structures formed by $TTR_{105-115}$ alone (Figure

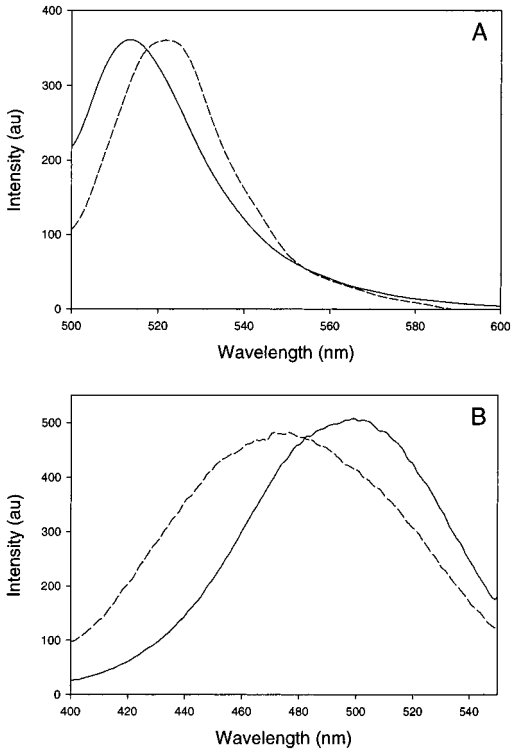

Figure 1. Fluorescence emission spectra of labeled peptide fibrils. Panel a: F5M-TTR_{10-19} incorporated into TTR_{10-19} fibrils (dashed line) is compared with F5M-TTR_{10-19} (solid line) in 20 mM sodium phosphate buffer, pH 7.0 at a final labeled peptide concentration of 0.3 μM. Panel b: dansyl-$TTR_{105-115}$ incorporated into $TTR_{105-115}$ fibrils (*dashed line*) is compared with dansyl-$TTR_{105-115}$ (solid line) in water at a final labeled peptide concentration of 0.9 μM. The fluorescence spectra have been normalized.

Table 1. Spectral Properties of Fluorescently Labeled Amyloid Fibrils

fluorophore	fibrils	λ_{max}[a] (nm)	$\Delta\lambda_{max}$[b]	anisotropy[c]
F5M-TTR_{10-19}		518		0.03
F5M-TTR_{10-19}	TTR_{10-19}	527	9	0.17
F5M-TTR_{10-19}	$TTR_{105-115}$	520	2	0.22
F5M-TTR_{10-19}	insulin	524	6	0.16
$TTR_{105-115}$-dansyl		502		0.02
$TTR_{105-115}$-dansyl	TTR_{10-19}	476	26	0.16
$TTR_{105-115}$-dansyl	$TTR_{105-115}$	472	30	0.13
$TTR_{105-115}$-dansyl	insulin	470	32	0.19

[a] The wavelength of maximum fluorescence emission. [b] The change in the wavelength of maximum fluorescence emission on incorporation of the labeled peptide into fibrils. [c] The fluorescence anisotropy, acquired at λ_{max}.

(10) MacPhee, C. E.; Dobson, C. M. *J. Mol. Biol.* **2000**, 297, 1203–1215.

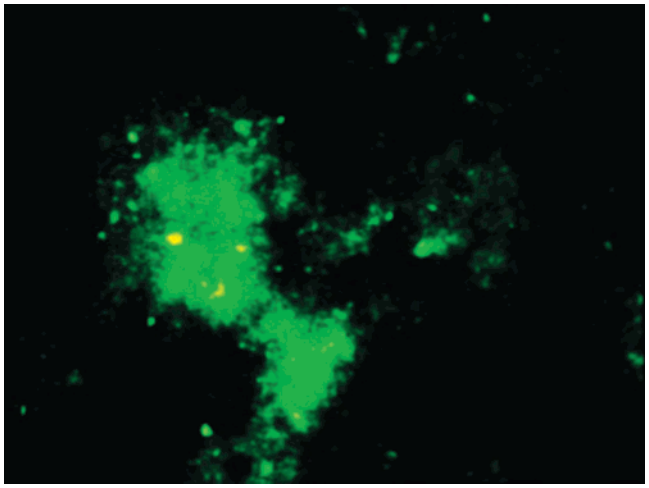

Figure 2. Fluorescence light microscopy of TTR_{10-19} amyloid fibrils containing 1% (w/w) dansyl-$TTR_{105-115}$. TTR_{10-19} fibrils containing dansyl-$TTR_{105-115}$ were prepared at a total of 10 mg/mL peptide in 10% (v/v) CH_3CN adjusted to pH 2 with TFA and incubated at 37 °C for 10 days. Fibrils were pelleted by centrifugation at 9500*g* for 15 min; the pellet was resuspended in H_2O pH 2, deposited on a glass slide, and imaged using fluorescence light microscopy.

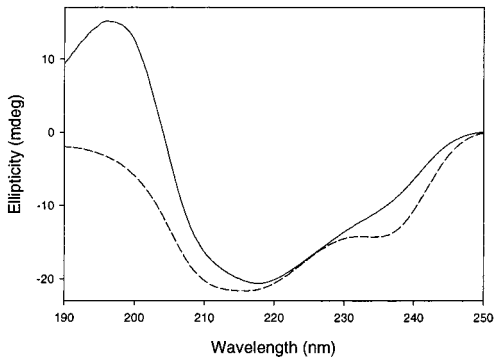

Figure 3. Change in the secondary structure of amyloid fibrils on doping with guest peptide. Circular dichroism spectroscopy of $TTR_{105-115}$ fibrils in the presence and absence of 1% (w/w) F5M-TTR_{10-19}. $TTR_{105-115}$ fibrils (dashed line) were generated by resuspending the peptide at 10 mg/mL in 20% CH_3CN at pH 2 and incubating for 24 h at 37 °C, followed by 7 days incubation at room temperature. Fibrils containing 1% (w/w) F5M-TTR_{10-19} (solid line). The 10 mg/mL peptide stock solution was incubated for 10 days at 37 °C in solution containing 10% CH_3CN.

4*a*), and we observe cofibrils with a regular periodic twist (Figure 4b,c). Fluorescence spectroscopy indicates little change in the spectral properties of the fluorescein moiety, which exhibits a red-shift of only ∼2 nm, but the anisotropy increases substantially to 0.22. These experiments together indicate that it is possible to generate cofibrils of two different peptides, strongly suggesting that the identity of the amino acid side chains is not critical for the ability of a polypeptide chain to form fibrils.

To establish the location of the fluorescent peptides doped into the fibril assemblies, we developed an immunogold labeling procedure. The fluorescein moiety provides a ready antigenic target for antibody binding that, on addition of a second antibody labeled with colloidal gold, can be detected by electron microscopy. This technique is similar in concept to that employed for identification of pathological proteins, by way of in situ staining of thin tissue sections.[11] Figure 5a shows

(11) Inoue, S.; Kuroiwa, M.; Saraiva, M. J.; Guimaraes, A.; Kisilevsky, R. *J. Struct. Biol.* **1998**, *124*, 1−12.

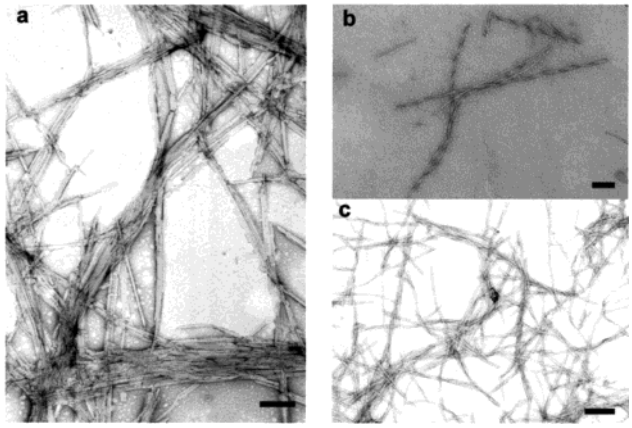

Figure 4. Change in the morphology of amyloid fibrils on doping with guest peptide. Negative stain electron microscopy of $TTR_{105-115}$ fibrils in the presence and absence of F5M-TTR_{10-19}. Panel a: electron micrographs of $TTR_{105-115}$ fibrils formed by incubation for 24 h at 37 °C, followed by 7-days incubation at room temperature in 20% CH_3CN pH 2. Panels b and c: electron micrographs of cofibrils consisting of $TTR_{105-115}$ containing 1% (w/w) F5M-TTR_{10-19}, formed by incubation for 10 days at 37 °C. Fibrils were negatively stained with uranyl acetate. Scale bar, 200 nm.

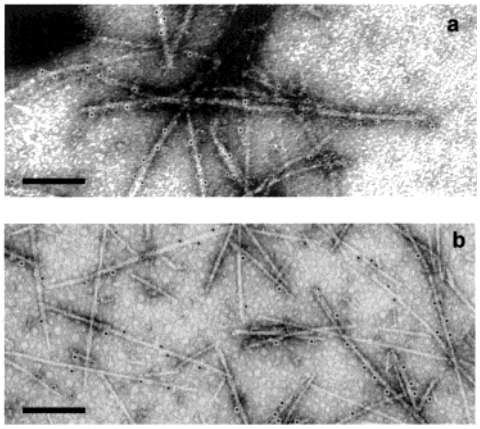

Figure 5. Immunogold labeling of TTR peptide cofibrils. Panel a: TTR_{10-19} fibrils containing 1% (w/w) F5M-TTR_{10-19}. Panel b: $TTR_{105-115}$ fibrils containing 1% (w/w) F5M-TTR_{10-19}. Scale bars, 200 nm.

TTR_{10-19} fibrils containing 1 wt % of F5M-TTR_{10-19}, probed with rabbit anti-fluorescein IgG, which was then probed with gold-labeled goat anti-rabbit IgG antibody. The 5-nm gold particles are observed to be associated with the various fibrils, whereas TTR_{10-19} fibrils alone did not elicit a reaction to the antibody. Measurement of the distances between successive gold clusters bound to the fibril indicates that the gold particles are distributed on average every 40−50 nm, but at irregular intervals along the fibril length. The hydrogen-bonding distance between peptides along the long axis of the fibril is 4.7 Å,[4] so the average distance between clusters suggests that the antigenic label is incorporated every 80−100 peptides. During fibrillogenesis, the fluorescently labeled peptide, which makes up ∼1 in every 100 of the peptide precursors, appears to be incorporated randomly into the growing fibril. Immunogold labeling of cofibrils made up of $TTR_{105-115}$ containing a trace of F5M-TTR_{10-19} are presented in Figure 5b. Gold particles are bound at approximately 40−60-nm intervals along the length of the fibril, again suggesting random insertion of the guest peptide into the growing fibril β-sheet scaffold. A further control experiment in which labeled peptide was added to preformed $TTR_{105-115}$ fibrils did not elicit antibody binding, indicating that F5M-

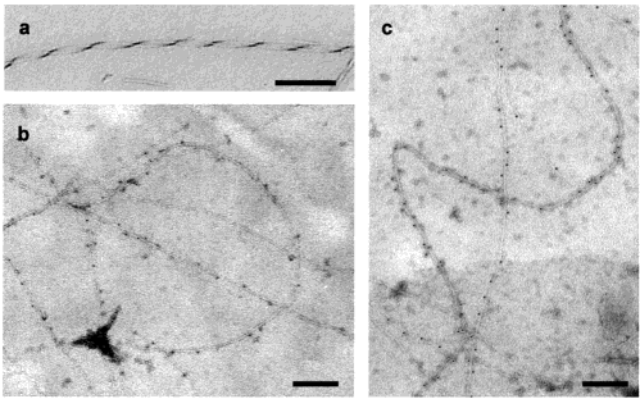

Figure 6. Electron microscopy and immunogold labeling of bovine insulin fibrils doped with guest peptide. Panel a: insulin fibrils containing F5M-TTR_{10-19}, negatively stained with uranyl acetate, to illustrate the regular nature of the helical twist along the length of the fibril. Scale bar, 100 nm. Panels b and c: immunogold labeled bovine insulin fibrils containing 1% (w/w) F5M-TTR_{10-19}. Scale bars, 200 nm.

TTR_{10-19} does not merely bind nonspecifically to fully assembled fibrils.

Incorporation of Labeled Peptides into Insulin Fibrils. An additional series of experiments was carried out to determine whether the fluorescently labeled peptides could be incorporated into fibrils assembled primarily from an unrelated protein sequence and, moreover, a sequence of 51 residues, much longer than that of the reporter peptides. The protein chosen for investigation was bovine insulin, which consists of two disulfide-linked chains in its largely helical native fold. The formation of fibrils from bovine insulin is well established and is readily achieved by heating the protein to high temperatures (>60 °C) at low pH.[12] Under these conditions, however, the rate of fibril formation by the insulin molecules is significantly faster than that observed for TTR_{10-19} and $TTR_{105-115}$, 7 h for completion of the process, whereas both peptides remain soluble for 48 h under similar conditions. Experiments revealed that the kinetics of fibril formation by the two protein species must be relatively evenly matched, otherwise the fluorescent species is not incorporated efficiently into the growing fibril. We therefore modified the conditions of fibril formation by insulin to adjust the rate of assembly to approximately that of fibril formation by the short peptides: pH 2.7 at 55 °C, under which conditions the fibrils formed over a period of 10 days. The peptides alone at the concentration used for cofibril formation (0.05 mg/mL) remained fully soluble over a period of 3 weeks under identical conditions.

Comparison of CD spectra acquired over the 10-day incubation period indicates the transition from the predominantly α-helical structure of bovine insulin to the β-sheet structure typical of amyloid fibril formation, as reported previously.[13] The resulting fibrils display a characteristic helical twist along the long axis of the fibril, repeating every ~60 nm (Figure 6a). Approximately 60% of the F5M-TTR_{10-19} sedimented with the fibrils on ultracentrifugation, and the fluorescence properties of the probe that colocalized with the fibrils were consistent with insertion of the fluorescein group into the fibril structure (6-nm spectral shift, anisotropy 0.16; Table 1). The fluorescence properties of purified cofibrils containing dansyl-$TTR_{105-115}$ were also consistent with insertion of the fluorophore into the insulin fibrils, with a 32-nm blue-shift in the wavelength of maximum emission to 470 nm and an increase in anisotropy to 0.19 (Table 1). More than 70% of the peptide was found in the pellet on centrifugation of the fibrils.

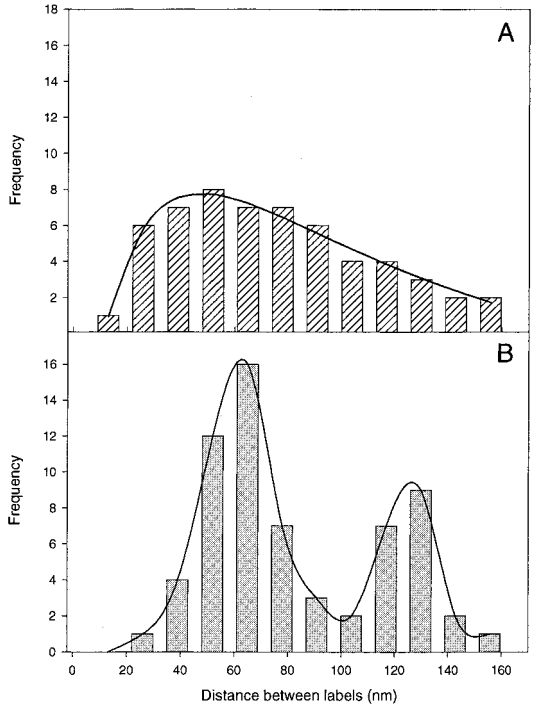

Figure 7. Periodic binding of anti-fluorescein IgG to insulin-TTR_{10-19} cofibrils. Panel a: histogram showing the distance (in nm) between colloidal gold particles bound to $TTR_{105-115}$ fibrils containing F5M-TTR_{10-19}. The distance between particles was measured from the image presented in Figure 5b. Panel b: histogram showing the distance (in nm) between colloidal gold particles bound to insulin fibrils containing F5M-TTR_{10-19}. The distance between particles was measured from the images presented in Figure 6b,c.

Panels b and c of Figure 6 show the results of immunogold labeling of insulin fibrils containing F5M-TTR_{10-19}. Again, gold clusters can be seen associated with the fibrils, indicating the incorporation of the labeled peptide, and there was no nonspecific binding of F5M-TTR_{10-19} on incubation of soluble peptide with preformed insulin fibrils. Unlike the cofibrils prepared with TTR_{10-19} or $TTR_{105-115}$ (Figure 7a), the binding of gold-labeled antibody to insulin-TTR cofibrils appears to exhibit a degree of regularity. The periodicity is presented as a histogram in Figure 7b, which indicates that the labeling occurs at ~60- and ~125-nm intervals. A possible interpretation of this result is the regular insertion of the peptide into the growing insulin fibrils: the helical twisting of insulin fibrils every 60 nm along the fiber axis (Figure 6a) is at least one structural phenomenon that repeats at regular intervals. The periodic binding of gold particles may represent insertion of the peptide into the growing insulin fibril only on fibril twisting. However, current models of fibril assembly indicate that protofilament substructures are formed first, which then associate and adopt a helical pitch only in the assembled fibril.[10,14] We therefore believe that the observed peridocity is due to the exposure of the antigen to the aqueous phase at intervals defined by the twisting of the fibril and that peptide incorporation into the growing protein fibril once again occurs randomly.

(12) Waugh, D. F. *J. Am. Chem. Soc.* **1946**, *68*, 247−250.

(13) Bouchard, M.; Zurdo, J.; Nettleton, E. J.; Dobson, C. M.; Robinson C. V. *Protein Sci.* **2000**, *9*, 1960−1967.

(14) (a) Harper, J. D.; Wong, S. S.; Lieber, C. M.; Lansbury, P. T. *Biochemistry* **1999**, *38*, 8972−8980.

Discussion

The current evidence that unrelated peptides can be incorporated into amyloid fibrils provides compelling support for a generic structure of these fibrils that is dictated not by side-chain-specific interactions but by the formation of a network of hydrogen bonds between the invariant groups that make up the polypeptide backbone. In correctly folded globular proteins, the backbone is involved in a series of stabilizing interactions and thus amyloid fibril formation is observed only following partial denaturation or destabilization of a stable tertiary structure[15] or the physiologically inappropriate generation of unstructured peptide fragments in vivo.[16] The identity of the amino acid side chains will affect the structure and stability of the protein precursor but will not dictate the fundamental β-sheet hydrogen-bonding network of the assembled fibril. Different side chains will pack together in different ways within the assembled sheet structure, as indeed is observed in globular structures.[17] It is likely that for some sequences particularly favorable contacts will be made between different side chains and result in more favorable packing interactions. Such sequences may therefore show high propensities to form fibrillar structures. But these propensities, and the stability of the fibrils under specific solution conditions, will also depend on the intrinsic properties of the soluble form of the polypeptide chain, such as its interaction with solvent and the stability of the globular structure. Moreover, the identity of the amino acid side chains will also influence the interactions between the unstructured regions that are thought to have an effect on the self-assembly of protofilaments into amyloid fibrils. In this way, different protein species may give rise to amyloid fibrils with differences in the detailed morphology but with a common underlying hydrogen-bonding β-sheet network.

The formation of mixed fibrils may also be of significance in diseases associated with amyloid deposition. It has been demonstrated that amyloid protein A (AA) amyloidosis in mice can be accelerated by the injection of preformed amyloid fibrils assembled from a number of peptide sources, including residues 20−29 of islet amyloid polypeptide (IAPP) and the sequences TTR_{10-19} and $TTR_{105-115}$ employed in this study.[18] This suggests that injection of fibrillar material could provide a seeding mechanism for the deposition of amyloid protein A. Cofibril formation is also consistent with the detection of both wild-type and mutant forms of transthyretin in FAP amyloid deposits[19] and the colocalization of apolipoprotein E with the Aβ-peptide implicated in Alzheimer's disease.[20] Mixed fibril deposition in vivo is statistically much less likely than the formation of fibrils from a single species, as the process of cofibril formation would require partial unfolding, degradation, or destabilization of two molecular species in the same location, processes that are rigorously controlled in the cell.

Non-native self-assembling peptide polymers have previously been synthesized, following careful design principles based on side-chain interactions, to form reversible and pH-dependent hydrogels, β-sheet peptide nanotubes that can act as nonspecific pores within membranes, β-sheet "nanotapes", and lamellar crystals.[21] The formation of amyloid fibrils of the type described in the present work requires no explicit design process since it is a fundamental property of the polypeptide backbone. The solubility, stability, and conformational properties of monomeric precursors will, however, vary with the specific sequence, allowing exploitation of a wide range of environments for fibril assembly. The side-chain interactions within β-sheets of different compositions will furthermore influence and modulate the physical properties and the morphologies of the resulting fibrils. We and others have observed the formation of amyloid fibrils as tubular structures with a hollow core, flat ribbonlike morphologies and twisted fibrils where the periodicity of the twist is dictated by the identity of the protein or peptide precursor; we have also noted the influence of the protein precursor on the average diameter and homogeneity of the resulting fibril population.[22] Moreover, previous work has indicated that fibril assembly can be reversed on modulation of the solvent environment,[10] suggesting their utility as chemically reversible and biodegradable gels. Indeed, it seems likely that the amyloid fibrils from native proteins and peptides are closely related to some of these artificially designed systems.

In addition to the 20 naturally occurring amino acids, manipulation of bacterial expression systems has enabled the incorporation of amino acids with unnatural side chains into the polypeptide chain,[23] thereby expanding the repertoire of chemical functionalities available for exploitation. By utilizing specific conjugation chemistries, amyloid fibrils may provide a rigid scaffold that can be covalently modified by the conjugation of fully folded and active proteinaceous enzymes or cofactors or nonprotein materials such as metals, chelating agents, or optically active compounds. Indeed, Krobitsch & Lindquist[24] have demonstrated the conjugation to an amyloidogenic protein species of an extrinsic protein that remains active even on induction of fibril assembly, suggesting that a functional native protein structure can be maintained independently of the formation of amyloid fibrils. Moreover, recognition of the fact that fibril assembly is a fundamental property of the polypeptide chain raises the possibility of employing these fibrillar arrays as structural building blocks in the development of novel biomaterials and nanostructures. Unlike the products of conventional organic polymerization processes, artificial proteins can be engineered with virtually absolute control of composition, chain length, sequence, and stereochemical purity.

(15) (a) McCutchen, S. L.; Lai, Z.; Miroy, G. J.; Kelly, J. W.; Colon, W. *Biochemistry* **1995**, *34*, 13527−13536. (b) Booth, D. R.; Sunde, M.; Bellotti, V.; Robinson, C. V.; Hutchinson, W. L.; Fraser, P. E.; Hawkins, P. N.; Dobson, C. M.; Radford, S. E.; Blake, C. C.; Pepys, M. B. *Nature* **1997**, *385*, 787−793.

(16) (a) Maury, C. P. *J. Clin. Invest.* **1991**, *87*, 1195−1199. (b) Haggqvist, B.; Naslund, J.; Sletten, K.; Westermark, G. T.; Mucchiano, G.; Tjernberg, L. O.; Nordstedt, C.; Engstrom, U.; Westermark, P. *Proc. Natl. Acad. Sci. U.S.A.* **1999**, *96*, 8669−8674. (c) Obici, L.; Bellotti, V.; Mangione, P.; Stoppini, M.; Arbustini, E.; Verga, L.; Zorzoli, I.; Anesi, E.; Zanotti, G.; Campana, C.; Vigano, M.; Merlini, G. *Am. J. Pathol.* **1999**, *155*, 695−702.

(17) Minor, D. L.; Kim, P. S. *Nature* **1996**, *380*, 730−734.

(18) Johan, K.; Westermark, G.; Engstrom, U.; Gustavsson, A.; Hultman, P.; Westermark, P. *Proc. Natl. Acad. Sci. U.S.A.* **1998**, *95*, 2558−2563.

(19) Ando, Y.; Ando, E.; Ohlsson, P. I.; Olofsson, A.; Sandgren, O.; Suhr, O.; Terazaki, H.; Obayashi, K.; Lundgren, E.; Ando, M.; Negi, A. *Amyloid* **1999**, *6*, 119−123.

(20) Sanan, D. A.; Weisgraber, K. H.; Russell, S. J.; Mahley, R. W.; Huang, D.; Saunders: A.; Schmechel, D.; Wisniewski, T.; Frangione, B.; Roses, A. D.; Strittmatter, W. J. *J. Clin. Invest.* **1994**, *94*, 860−869.

(21) (a) Petka, W. A.; Harden, J. L.; McGrath, K. P.; Wirtz, D.; Tirrell, D. A. *Science* **1998**, *281*, 389−392. (b) Ghadiri, M. R.; Granja, J. R.; Buehler, L. K.; *Nature* **1994**, *369*, 301−304. (c) Aggeli, A.; Bell, M.; Boden, N.; Keen, J. N.; Knowles, P. F.; McLeish, T. C.; Pitkeathly, M.; Radford, S. E. *Nature* **1997**, *386*, 259−262. (d) Krejchi, M. T.; Atkins, E. D.; Waddon, A. J.; Fournier, M. J.; Mason, T. L.; Tirrell, D. A. *Science* **1994**, *265*, 1427−1432.

(22) (a) Jiménez, J. L.; Guijarro, J. I.; Orlova, E.; Zurdo, J.; Dobson, C. M.; Sunde, M.; Saibil, H. R. *EMBO J.* **1999**, *18*, 815−821 (b) Goldsbury, C. S.; Cooper, G. J.; Goldie, K. N.; Muller, S. A.; Saafi, E. L.; Gruijters, W. T.; Misur, M. P.; Engel, A.; Aebi, U.; Kistler, J. *J. Struct. Biol.* **1997**, *119*, 17−27.

(23) (a) van Hest, J. C.; Tirrell, D. A. *FEBS Lett*. **1998**, *428*, 68−70. (b) Sharma, N.; Furter, R.; Kast, P.; Tirrell, D. A. *FEBS Lett.* **2000**, *467*, 37−40.

(24) Krobitsch, S.; Lindquist, S. *Proc. Natl. Acad. Sci. U.S.A.* **2000**, *97*, 1589−1594.

The vast array of possible combinations of the 20 naturally occurring amino acids suggests innumerable possibilities for novel biomaterials. The production of fibrils with fluorescent properties in the present work indicates the ability to design nanomaterials with potentially important physical properties for a wide range of applications.

Conclusion

In the current study, we have shown that it is possible to form amyloid fibrils consisting of two distinct molecular species that coassemble within the β-sheet array that makes up the core of these structures. This evidence that fibril assembly is not dependent on the identities and properties of the amino acid side chains in the polypeptide sequence provides strong evidence that fibrillogenesis is a fundamental property of all proteins, rather than a pathogenic process restricted to just a few unusual sequences. Additionally, by incorporating unusual chemical groups into the fibrils we have demonstrated that these fibril assemblies may be functionalized, suggesting their potential use as novel biomaterials with a wide range of possible applications.

Experimental Section

Peptide Synthesis. TTR_{10-19} (CPLMVKVLDA) and $TTR_{105-115}$ (YTIAALLSPYS) were synthesized on an Applied Biosystems 430A automated peptide synthesizer using standard Fmoc chemistry, within the Oxford Centre for Molecular Sciences. After cleavage from the support, the peptides were purified by RP-HPLC on a Beckman System Gold HPLC using either an analytical Brownlee 4.6 × 30 mm C-8 reversed-phase column or a preparative Vydac 10 × 250 mm C-18 reversed-phase column. Fractions eluting from the column were analyzed by MALDI-TOF mass spectrometry, and fractions of the desired molecular weight were pooled and lyophilized.

Peptide Labeling. (1) TTR_{10-19} Labeling with Fluorescein. The N-terminal cysteine residue of TTR_{10-19} was the target for labeling by the thiol-reactive fluorophore fluorescein-5-maleimide (F5M; Molecular Probes, Eugene, OR). TTR_{10-19} was resuspended at 1 mg/mL in H_2O, and the cysteine residue reduced by the addition of a 10-fold molar excess of tris(2-carboxyethyl) phosphine (TCEP; Molecular Probes) and incubation for 1 h at room temperature. F5M in DMSO was added to the peptide solution to give a 10-fold molar excess of fluorophore over peptide in a final concentration of 10% DMSO. Under these conditions, TTR_{10-19} was fully soluble. The mixture was incubated overnight at 4 °C to ensure maximum labeling. The labeling mixture was then applied to a disposable SepPak C-18 reversed-phase chromatography column (Waters, Milford, MA) and washed with H_2O/CH_3CN (90:10 v/v). TCEP and unreacted label eluted in the wash. The peptide was then eluted from the column with H_2O/CH_3CN (40:60 v/v), and a mixture of labeled and unlabeled peptide was detected by MALDI-TOF mass spectrometry. The labeling efficiency was estimated at ~70% by mass spectrometry and also by absorption measurements, assuming an extinction coefficient of 83 000 at 492 nm.

(2) $TTR_{105-115}$ Labeling with Dansyl Chloride. The N-terminal amino group of $TTR_{105-115}$ was the target for labeling with dansyl chloride (Molecular Probes). $TTR_{105-115}$ was resuspended at 1 mg/mL in H_2O/CH_3CN (80:20 v/v). Dansyl chloride in DMSO was added to the peptide solution to give a 10-fold molar excess of fluorophore over peptide in a final concentration of 10% DMSO. The pH was adjusted manually to 9.0 with the addition of ammonia. Under these conditions, $TTR_{105-115}$ was fully soluble. The mixture was incubated for 2 h at room temperature to ensure maximum labeling. The labeling mixture was then applied to a disposable SepPak C-18 reversed-phase chromatography column (Waters) and washed with H_2O. There was no detectable elution of material during the wash step. The peptide was then eluted from the column with H_2O/CH_3CN (50:50 v/v), and a mixture of labeled and unlabeled peptides was detected by MALDI-TOF mass spectrometry. Unreacted dansyl chloride did not elute from the column under these conditions. The labeling efficiency was estimated at ~80% by mass spectrometry and also by absorption measurements, assuming an extinction coefficient of ~4000 at 370 nm.

Fibril Formation. TTR_{10-19} fibrils, in the presence and absence of F5M-TTR_{10-19}, were generated by resuspending the peptide at 10 mg/mL in H_2O at pH 2.0 and incubating at room temperature for 5 days. In fibrils containing the labeled species, the molar ratio of unlabeled to labeled peptide was 100:1.

$TTR_{105-115}$ fibrils, in the presence and absence of dansyl-$TTR_{105-115}$, were generated by resuspending the peptide at 10 mg/mL in CH_3CN/H_2O (20:80 v/v) at pH 2 and incubating at 37 °C for 7 days. In fibrils containing the labeled species, the molar ratio of unlabeled to labeled peptides was 100:1.

Bovine insulin (Sigma Chemical Co., MO) fibrils were generated by resuspending the protein at 11.5 mg/mL (2 mM) in H_2O at pH 2.5 and incubating the suspension at 70 °C for 1 h. The protein solution was plunged into liquid N_2 and then returned to 70 °C for a further 4 h.

Cofibril Formation. Both TTR_{10-19} fibrils containing dansyl-$TTR_{105-115}$ and $TTR_{105-115}$ fibrils containing F5M-TTR_{10-19} were prepared at a molar ratio of unlabeled to labeled peptides of 100:1. The stock solution containing a total of 10 mg/mL peptide was prepared in CH_3CN/H_2O (10:1 v/v) adjusted to pH 2 with H_2O and incubated at 37 °C for 10 days. Bovine insulin was prepared as a stock solution of 9.7 mg/mL in H_2O at pH 2.7, containing a molar ratio of insulin to labeled peptide species (dansyl-$TTR_{105-115}$ or F5M-TTR_{10-19}) of 40:1. The solution was incubated at 55 °C for 10 days. Fibril formation was assessed by CD spectroscopy and by EM.

Circular Dichroism Spectroscopy. CD spectra were acquired on a Jasco model J-720 spectropolarimeter using a 0.1-cm path length quartz cuvette. The temperature was kept constant at 25 °C by use of a circulating water bath. Each spectrum represents the average of four scans acquired at 0.5-nm intervals between 200 and 250 nm, with a response time of 4 s. The data are expressed in millidegrees rather than mean residue ellipticity due to the difficulty associated with accurately determining the absolute concentration of an aggregated peptide. For this reason, it was not possible to accurately determine the amount of β-sheet structure within the complexes. Furthermore, in all cases, the absorption of the sample was monitored concurrently to the circular dichroism signal, to avoid possible distortion of the spectrum due to light scattering or absorption flattening phenomena.

Fluorescence Spectroscopy. Fluorescence spectroscopic measurements were performed on a Perkin-Elmer LS50B luminescence spectrometer equipped with a fast filter accessory to enable anisotropy measurements. Quartz cuvettes with a 1-cm path length were employed throughout. The temperature was kept constant at 25 °C by use of a circulating water bath. Slit widths were 2.5 and 10 nm unless otherwise stated. Samples containing fluorescein were excited at 490 nm, with emission detected between 500 and 600 nm. Samples containing dansyl chloride were excited at 370 nm and the emission measured between 400 and 550 nm. The absorbance of each sample at the excitation wavelength was also monitored using a Cary-3 absorbance spectrometer, to avoid scattering artifacts and inner filtering effects. All anisotropy measurements were monitored over 10 s to rule out photobleaching phenomena and then averaged.

Electron Microscopy. Electron micrographs of amyloid fibrils were acquired on a JEOL JEM-1010 transmission electron microscope at 80-kV excitation voltage. A 2-μL sample of peptide at a concentration of 10−60 μg/mL was applied to Formvar- and carbon-coated copper grids. The fibrils were washed by the successive addition of three 10-μL aliquots of water, each wash step followed by drying with filter paper. The fibrils were stained with by the addition of 10 μL of uranyl acetate (1% w/v) and immediately dried with filter paper.

Immunogold Labeling. A 2-μL aliquot of peptide at a concentration of 10−60 μg/mL was applied to Formvar- and carbon-coated grids. After 1 min, the solution was blotted with filter paper, and the grids blocked with Hanks' balanced salt solution (HBSS; Sigma Chemical Co, St. Louis, MO) containing 1% (w/v) ovalbumin for 5 min. Sample treatment was performed by inverting the grids onto a 20-μL droplet of the appropriate solution placed on a sheet of laboratory Parafilm. The grids were incubated with the primary antibody (rabbit anti-

fluorescein IgG diluted 1/10 into HBSS, Molecular Probes) for 30 min at room temperature before washing three times for 5 min with the blocking solution (HBSS/ovalbumin). The secondary antibody, colloidal gold-labeled goat anti-rabbit IgG (Sigma Chemical Co.), was diluted 1/10 in HBSS and applied to the grids for 30 min. The grids were washed three times for 10 min in blocking solution, fixed in 0.5% (v/v) glutaraldehyde for 10 min, washed with H_2O for 1 min, and stained with 0.5% (w/v) uranyl acetate.

Acknowledgment. The Oxford Centre for Molecular Sciences is supported by the U.K. Biotechnology and Biological Sciences Research Council, the Engineering and Physical Sciences Council, and the Medical Research Council. C.E.M is a Royal Society Dorothy Hodgkin Research Fellow. The research of C.M.D. is supported in part by the Wellcome Trust. We thank Maureen Pitkeathly for the synthesis and purification of TTR_{10-19} and $TTR_{105-115}$, Anne Clark for instruction and aid with electron microscopy and advice on immunolabeling, and David Harvey for the use of his LaserMAT MALDI-TOF mass spectrometer.

JA0029580